Numerical analysis of atherosclerosis and aneurysm in carotid bifurcations using computational fluid dynamics.

ASIM, T., SENDANAYAKE, I. and MISHRA, S.

2013

Proceedings of the Fortieth National Conference on Fluid Mechanics and Fluid Power
December 12-14, 2013, NIT Hamirpur, Himachal Pradesh, India

FMFP2013_178

Numerical Analysis of Atherosclerosis and Aneurysm in Carotid Bifurcations using Computational Fluid Dynamics

Taimoor Asim
University of Huddersfield
Huddersfield, UK
taimoor.asim@hud.ac.uk

Isuru Sendanayake
University of Huddersfield
Huddersfield, UK
u0857384@unimail.hud.ac.uk

Shashwat Mishra
Greenhead College,
Huddersfield, UK
shashwat.mishra95@hotmail.com

ABSTRACT

Atherosclerosis and Aneurysm are some of the conditions in patients suffering from vascular diseases. These vascular defects can cause severe damage to cardiovascular system (CVS), if not properly diagnosed. The advent of advanced numerical and computational techniques has enabled the researchers to accurately design and simulate the flow of blood through the complex flow systems. Current state of published research is mostly based on simplified modelling tools and qualitative analysis that is limited to macro level description of the flow field. There is a need to diagnose the flow structure at micro level in order to carry out hemodynamic analysis of such defects. Several cardiovascular models of a bifurcation in the carotid artery have been generated using Computational Fluid Dynamics based techniques in the present investigation. These models represent healthy and defective carotid bifurcations, where the defective bifurcations represent atherosclerotic and aneurysm conditions. It has been observed that the defects in the carotid bifurcation affect local Wall Shear Stress WSS) significantly. The magnitude of wall shear stress has been shown to be crucial in ulceration and plaque formation.

Keywords: Computational Fluid Dynamics (CFD), Carotid Bifurcation, Atherosclerosis, Aneurysm, Wall Shear Stress (WSS)

1. INTRODUCTION

Human cardiovascular system comprises of three main components i.e. heart, lungs and arteries. The circulation of blood within the CVS takes place through a sophisticated and a very well evolved

system of arteries. According to the British Heart foundation, in year 2011, almost 160,000 people in the UK died from cardiovascular diseases, and almost 74,000 of those deaths were a direct result of coronary heart diseases. Hence, a lot of attention is being paid nowadays to understand the mechanics of these conditions for better diagnostic purposes.

One of the most common diseases of the CVS is atherosclerosis in which carotid bifurcation becomes partially blocked due to the gradual build-up of fatty deposits around the internal wall of the artery. This restricts the blood flow within this artery, increasing the local wall shear stress, and hence poses a serious life threat to the patient by significantly increasing the chances of a stroke. Another common disease of the CVS is known as aneurysm in which the carotid bifurcation forms a bulge which eventually tears, resulting in internal bleeding.

According to Jiang et al., 2000 blood vessels are under the influence of two primary hemodynamic forces; the circumferential force and the wall shear stress (WSS). The circumferential force is originated as a result of the blood pressure acting on the walls of the arteries, whereas the wall shear stress is a result of the shearing forces being generated by the viscous flow of blood along the walls of the arteries. The study presented here focuses on the effects of the wall shear stress, being the most useful parameter in the analysis of flow field within carotid bifurcations.

The effects of stenosis (blockage due to atherosclerosis) and aneurysm, in the carotid bifurcations, have been studied by many researchers in the past decade. Steinman et al., 2002 have numerically analysed the effects of stenosis in human carotid bifurcations on various flow properties of blood such as flow velocity, flow rate and WSS. Increase in time-averaged WSS, in the stenosed region, has been observed in both the studies. Marshall et al., 2004 have also numerically analysed various atherosclerotic conditions and have shown that the time-averaged WSS for a normal carotid bifurcation can be higher than for a stenosed bifurcation. The similar observations have been observed by Martin et al., 2009.Milos et al., 2011 has compared the effectiveness of neural network and k-nearest neural network (k-NN) models for the prediction of WSS in various aneurysms. It has been shown that neural network model predicts the WSS with better accuracy as compared to k-NN model. Dong et al., 2013 have carried out detailed numerical investigations on carotid bifurcations being affected by various atherosclerotic conditions. Time averaged WSS, oscillatory shear index and relative resistance time have been analysed using CFD during one cardiac cycle. It has been shown that affected carotid bifurcation experiences a high time averaged WSS which leads to a high risk of plaque erosion.

Various researchers have shown that WSS is an important parameter in understanding local hemodynamics. However, most of the works take into account area average and/or time average WSS in analysing local hemodynamics on the regions affected by atherosclerosis and aneurysm. In this work, novel predictor equations have been developed that can quantify the peak, maximum and minimum WSS at a given time in a cardiac cycle and thus provide quantitative flow information at the micro level to link flow properties with defect conditions.

2. NUMERICAL MODELLING

In order to analyse the effects of atherosclerosis and aneurysm in carotid bifurcations, various CAD models have been developed that represent both the healthy and the affected bifurcations (Fig. 1). The

dimensions shown in Fig. 1(a) have been taken from Dong et al., 2013, who have taken it from a patient using MRI scanner. The various atherosclerotic models of the bifurcation represent 10% to 90% stenosis (Fig. 1(b)). For aneurysm, two different lengths of 4mm and 8mm for the affected region have been considered in the present study, and an area increase in the range of 25% to 125% has been specified for each length (Fig. 1(c)).

Three dimensional Navier-Stokes equations, along with the continuity equation, have been solved for the laminar flow of blood within the bifurcations. The equations have been solved in an iterative manner with stringent convergence criteria.

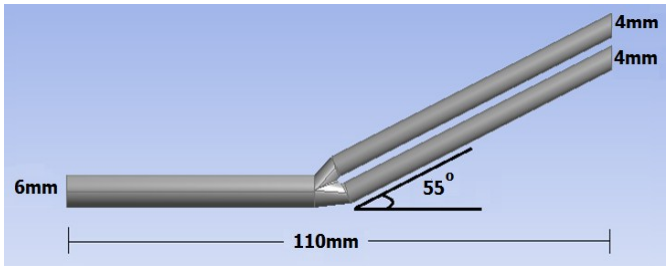

(a)

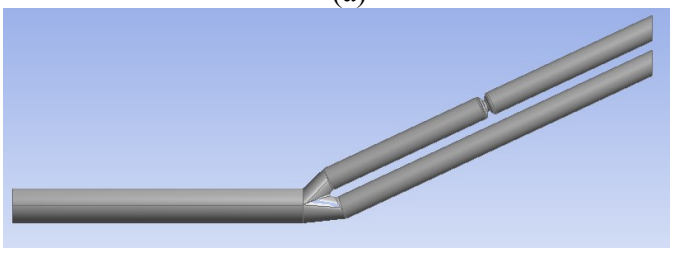

(b)

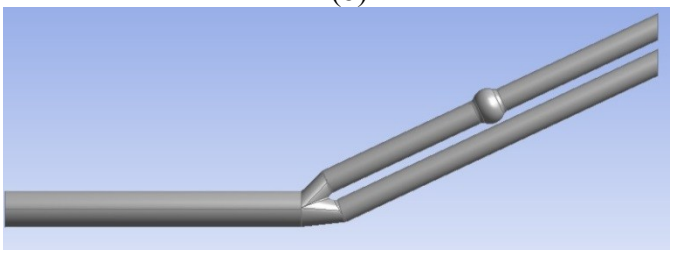

(c)

Figure 1. Various Carotid Bifurcation models (a) Healthy (b) 50% Atherosclerosis (c) 4mm-100% Aneurysm

For simplicity in computations, the walls of the bifurcations have been modelled as rigid walls with no-slip boundary condition. Pressure profile for a complete cardiac cycle has been obtained from Dong et al., 2013, as shown in Fig. 2. It can be seen that the pressure varies from 11,000Pa to 15,500Pa within one cardiac cycle. Hence, an operating gauge pressure of 10,000Pa has been prescribed within the computational domain.

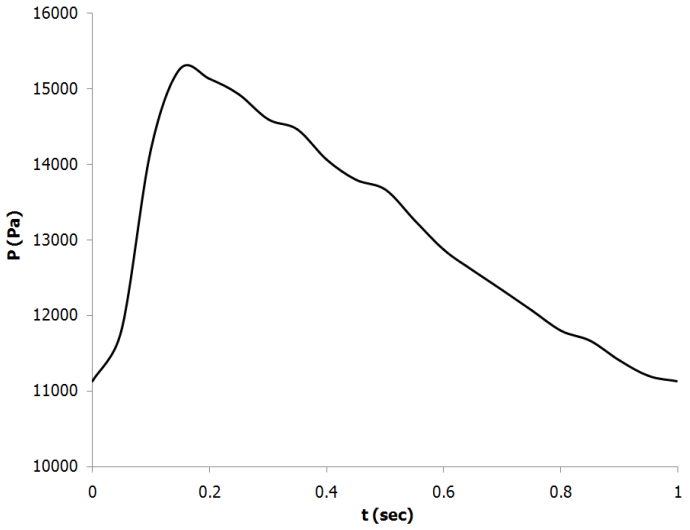

Figure 2. Pressure variations in blood during one cardiac cycle

Using multiple regression analysis, an expression has been developed (Eq. (1)) that generates the pressure profile with an average accuracy of 93%. This expression has been used as a user defined function at the pressure inlet boundary of the carotid bifurcation to simulate the transient flow of blood.

$$P = (139236 * t^6) - (340429 * t^5) + (218149 * t^4) + (75686 * t^3) - (136542 * t^2) + (44292 * t) + 791 \quad (1)$$

3. RESULTS AND ANALYSIS

Spatio-temporal discretisation studies have been carried out in order to accurately predict the local WSS in the affected region. These studies are an integral part of CFD based testing, so that the results are independent of mesh size used and time step size considered. The following sections present the results from these studies, as well as the numerical analysis of atherosclerosis and aneurysm.

3.1 Spatial Discretisation

In order to accurately predict the WSS in carotid bifurcations, the results should be independent of the mesh size used. Hence, a mesh independence study has been carried out in the present study. Two meshes have been generated consisting of 1million and 2million elements respectively within the flow domain. After one cardiac cycle, area weighted average WSS has been computed within the flow domain. It has been shown in Table 1 that the difference in average WSS between the two meshes is 1.18% for maximum stenosis of 90% and 2.12% for most severe aneurysm considered in the present study. Hence, the mesh with 1million mesh elements has been used to carry out further analysis.

An important point to mention at this point is that WSS acts in the near wall region only and hence the mesh elements needs to be concentrated in this region. This ensures that the flow parameters have been resolved accurately. Thus, 10 inflation layers have been used to accurately model the near wall region, for both atherosclerosis and aneurysm.

Table 1. Variation in Area Weighted Average WSS for different mesh sizes

Number of Mesh Elements	Average WSS for 90% Atherosclerosis	Difference w.r.t. 1 million Mesh Elements	Average WSS for 4mm-100% Aneurysm	Difference w.r.t. 1 million Mesh Elements
(-)	(Pa)	(%)	(Pa)	(%)
1 million	8.83		16.47	
2 million	8.93	1.18	16.82	2.12

3.2 Temporal Discretisation

To accurately resolve transient flow parameters, it is essential to perform temporal discretisation, or time step independence study. This ensures that the numerical results obtained are independent of time steps. In the present study, three different time step sizes of 0.1sec, 0.05sec and 0.025sec have been considered, and the results analysed. Area weighted average WSS has been recorded throughout the iterative process, for both 90% atherosclerosis and 4mm-125% aneurysm. It can be seen in Fig. 3 that the maximum difference in average WSS, among the time scales used, occurs at the peak of the pressure cycle i.e. at 0.3sec.

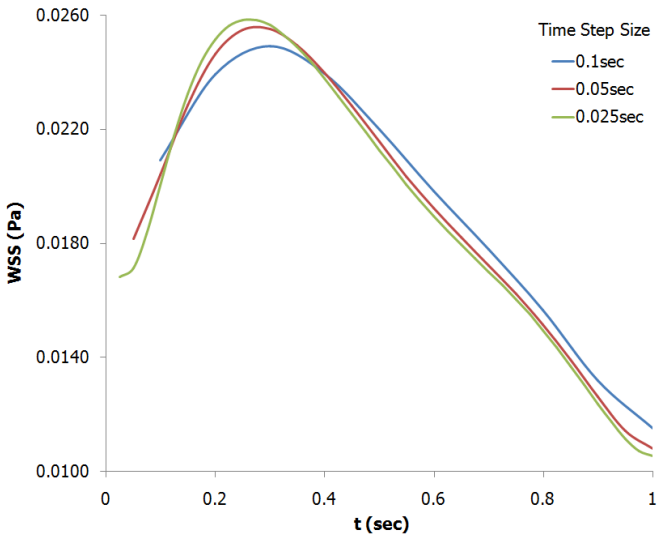

(a)

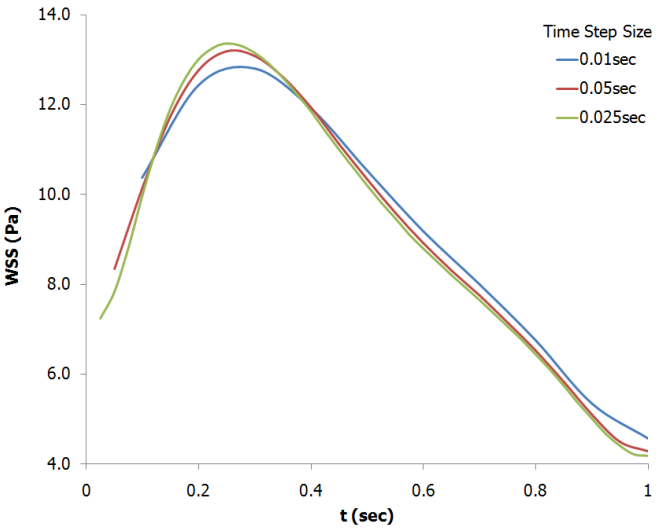

(b)

Figure 3. Variations in Area Weighted Average WSS at different time step sizes for (a) 90% Atherosclerosis (b) 4mm-125% Aneurysm

Table 2 shows the differences in the average WSS between different time step sizes (Δt) at 0.3sec. It can be seen that for 90% atherosclerosis, the difference between 0.1sec and 0.05sec time steps used is 2.11%, whereas this difference is 0.54% between 0.05sec and 0.025sec time steps. Furthermore, for 4mm-125% aneurysm, the difference between 0.1sec and 0.05sec time steps is 3.68%, whereas this difference is 1.31% between 0.05sec and 0.025sec time steps. Hence, a time step size of 0.05sec has been used to carry out further analysis in this study.

Table 2. Variation in Area Weighted Average WSS for different time step sizes

Δt	Average WSS in 90% Atherosclerosis	Difference w.r.t. 0.1sec	Average WSS in 4mm-125% Aneurysm	Difference w.r.t. 0.1sec
(sec)	(Pa)	(%)	(Pa)	(%)
0.1	12.8		23.63	
0.05	13.07	2.11	24.5	3.68
0.025	13.14	0.54	24.82	1.31

3.3Atherosclerosis

Figure 4 depicts the variations in the average WSS on the central plane within the carotid bifurcation having affected by 90% atherosclerosis. . It can be seen in Fig. 5 that there are considerable variations in the local WSS along the length of the stenosed region, suggesting that along the length of the affected region, local WSS is not uniform. From both Figs. 5(a) and 5(b), it can be seen that maximum WSS acts at the throat of the stenosed region, with a bias towards the entrance of the stenosis.

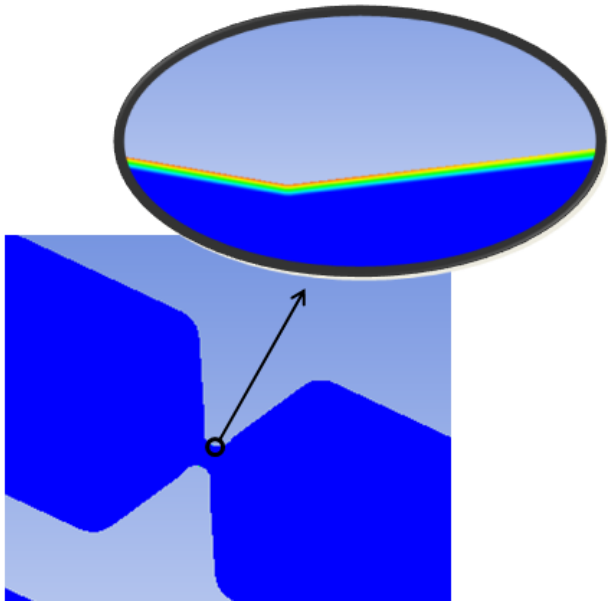

Figure 4. WSS at 90% Atherosclerosis

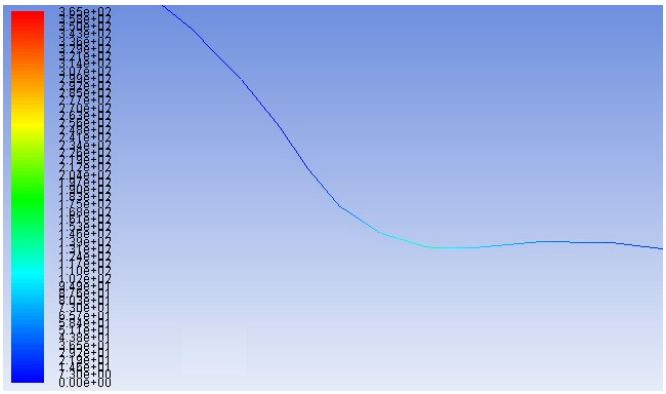

(a)

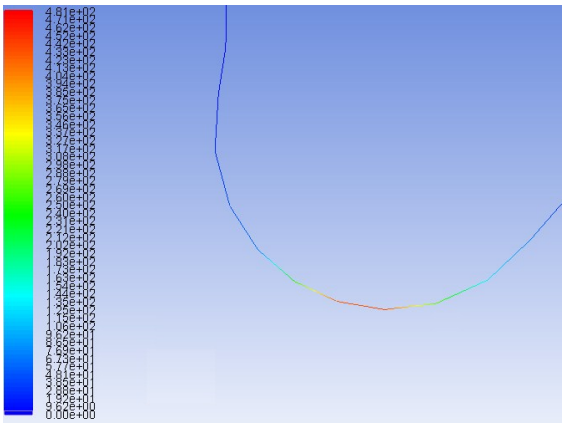

(b)

Figure 5. Variations in WSS for different Atherosclerotic conditions (a) 10% (b) 90%

In order to accurately evaluate the local WSS in the stenosed region, a curve has been generated for each atherosclerotic condition along the boundary wall of the affected region. Variations in the WSS at 0.3sec of the cardiac cycle (corresponding to maximum WSS) have been plotted along this curve, as shown in Fig. 6, where L represents the curve length. It is evident from Fig. 5that the maximum WSS acts in the throat region, and there is a bias towards the entrance side of the stenosed region. It can be clearly seen that the maximum WSS occurs at 30% of the curve length for the various atherosclerotic conditions considered in the present study.

It can be seen in Fig. 6 that as the severity of atherosclerosis increases from 10% to 40%, the WSS increases up to 500Pa. For 40%, 50% and 60% atherosclerosis, the maximum WSS remains the same, while for 70%, 80% and 90% atherosclerosis, the local maximum WSS remains constant at a value of 465Pa.

The initial increase in maximum WSS from 10% to 40% atherosclerosis is evident from the fact that as the severity of the stenosed region increases, the effective flow area reduces. This in-turn accelerates the flow at the throat, increasing the WSS. WSS is defined as:

$$WSS = \mu * \left(\frac{\partial u}{\partial y}\right)_{y=0} \quad (2)$$

where μ is the dynamic viscosity of blood, u is the local axial velocity of blood and y is the distance from the wall. Hence, increase in local axial velocity near the wall increases the WSS.

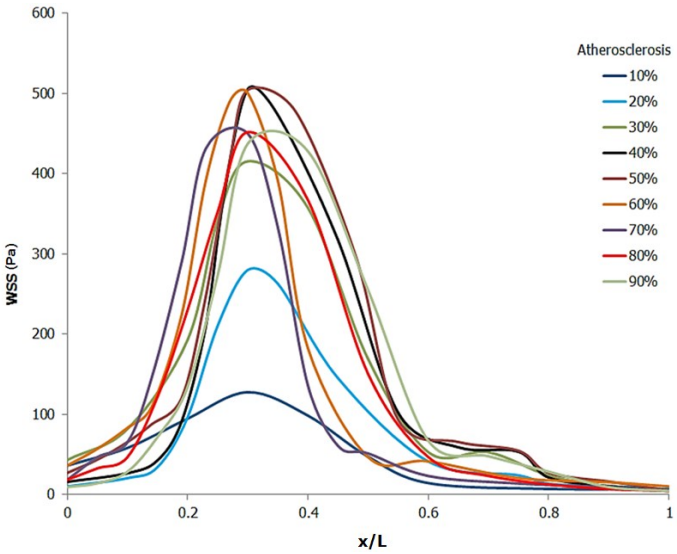

Figure 6. Variations in WSS for different Atherosclerotic conditions at 0.3sec

However, from 70% onwards, it has been observed that the WSS decrease. In order to investigate this phenomenon, axial velocity profiles at the throat of the stenosed region have been plotted for various atherosclerotic conditions, at 0.3sec of the cardiac cycle (Fig. 7). It can be clearly seen that for 10% and 90% atherosclerotic conditions, the axial velocity profiles resemble the ones usually observed for laminar flows. However, for 30% and 50% atherosclerotic conditions, the axial velocity profiles are quite different, and have flatter velocity profile. At 90% condition, however, the velocity gradient near the wall has reduced which shows increased effects of secondary flows.

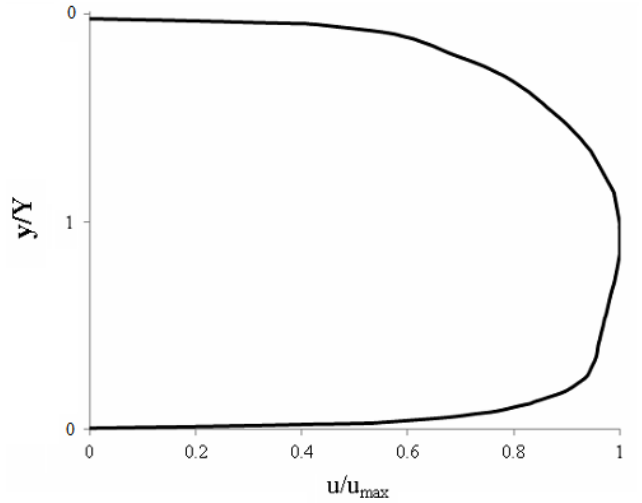

(a)

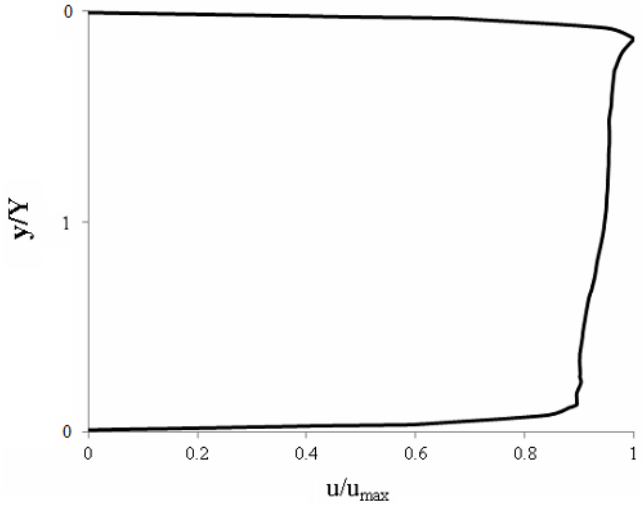

(b)

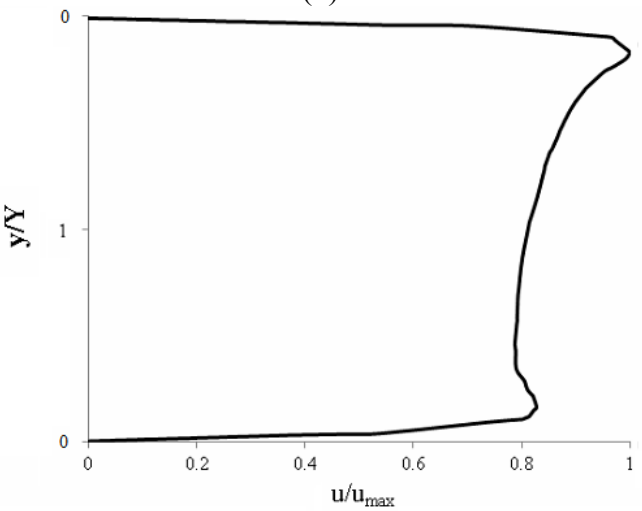

(c)

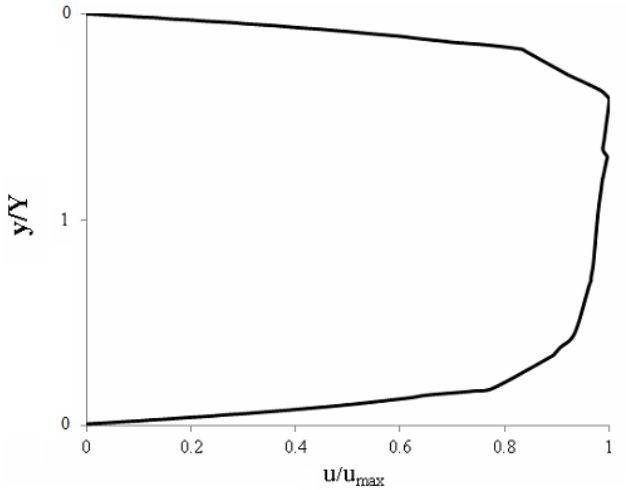

(d)

Figure 7. Variations in axial velocity profiles for various atherosclerotic conditions at 0.3sec (a) 10% (b) 30% (c) 50% and (d) 90%

Further analysing atherosclerosis in carotid bifurcations, Fig. 8 depicts the variations in normalised peak WSS with respect to various atherosclerotic conditions at the start, peak and the end of the cardiac cycle. The peak WSS acting on the affected region, at any given time, has been normalised with the average WSS acting along the curve length at the same time. It can be seen in Fig. 8 that normalised peak WSS increases as the severity of atherosclerosis increases. There is an increase of 81%, 45% and 73% in normalised peak WSS between 10% and 90% atherosclerosis at 0.05sec, 0.3sec and 1sec respectively. This suggests that peak WSS, in comparison with average WSS, have more pronounced effects on the affected region at the start and the end of the cardiac cycle as compared to the peak of the cardiac cycle.

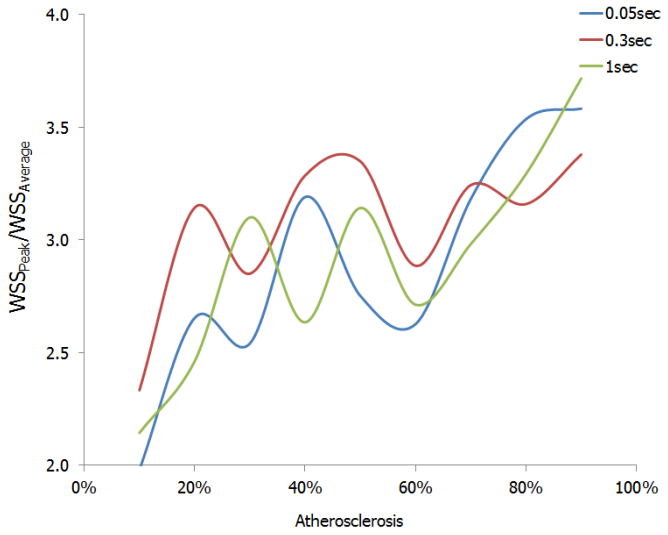

Figure 8. Variations in normalised peak WSS for different Atherosclerotic conditions

Figure 9 depicts the variations in normalised WSS during one complete cardiac cycle, for various atherosclerotic conditions considered in the present study. It can be seen that as the severity of the stenosed region increases, normalised peak WSS also increases.

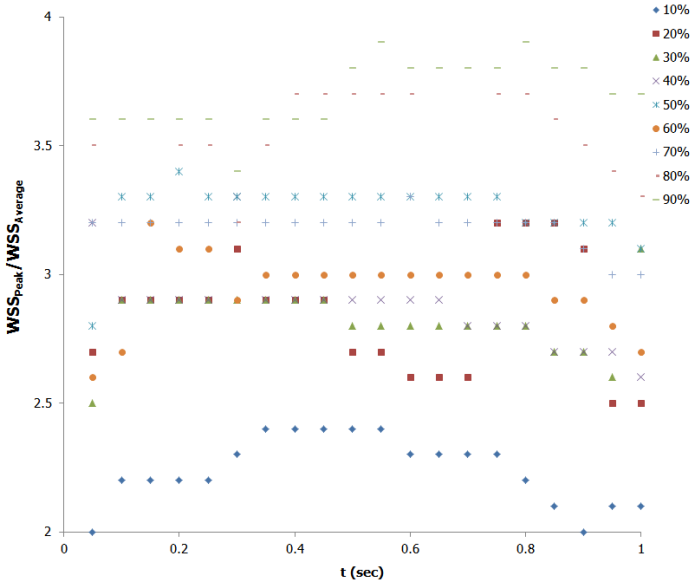

Figure 9. Variations in normalised peak WSS during a cardiac cycle for various atherosclerotic conditions

The results presented in Fig. 9 have been used to develop a novel expression for the prediction of normalised peak WSS acting on the region affected by atherosclerosis.

$$\frac{WSS_{Peak}}{WSS_{Avearge}} = 1 + (0.66\ \frac{t}{t_{avg}}^{0.0025}\ AT^{0.3}) \quad (3)$$

In the developed equation, t_{avg} is the average time for one complete cardiac cycle, which is 1sec in the present study, and AT corresponds to severity of atherosclerosis (in %). It can be seen that severity of atherosclerosis strongly influences the peak WSS.. Figure 10 presents the validity of Eq. (3). It can be seen that more than 85% of the data obtained from CFD, lies within ±15% error band of Eq. (3). Hence, Eq. (3) predicts the normalised peak WSS in the region affected by atherosclerosis, at a given time during a cardiac cycle, with reasonable accuracy.

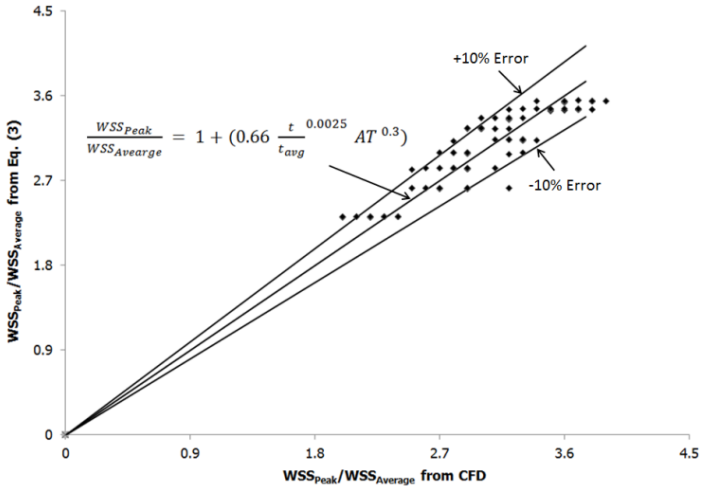

Figure 10. Validation of Eq. (3)

3.4 Aneurysm

In order to analyse the effects of aneurysm in carotid bifurcations, various models have been developed that represent their severity. In the present study,

aneurysms have been represented as, for example, 4mm-125%, where 4mm corresponds to the length of the affected region and 125% corresponds to the percentage area increase. Variations in pressure, at the central plane in carotid bifurcations, have been shown in Fig. 11 for 4mm-125% and 8mm-125%. It can be seen that the flow structure within the bifurcation is quite uniform as compared to atherosclerosis, and hence it is expected that the local WSS is considerably lower in aneurysms.

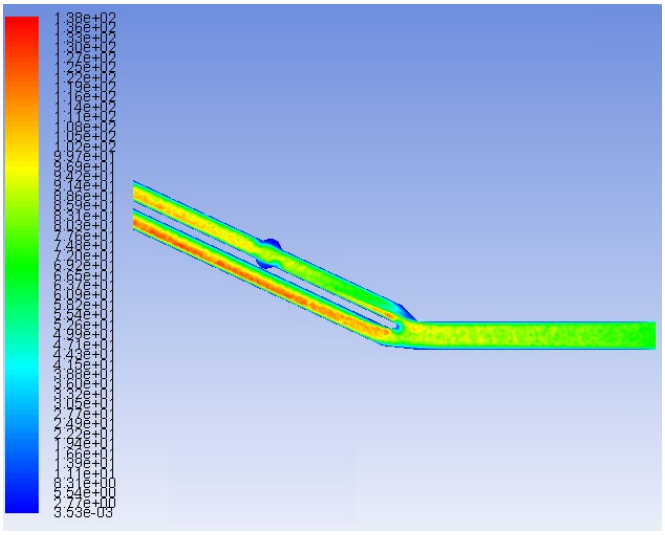

(a)

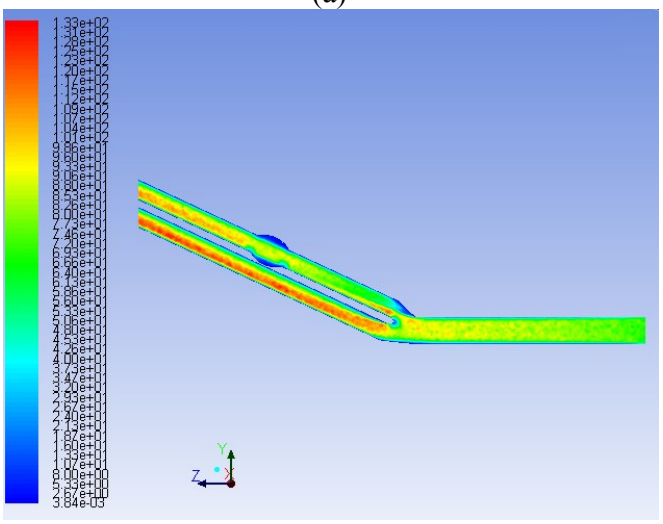

(b)

Figure 11. Pressure variations for different Aneurysms (a) 4mm-125% (b) 8mm-125%

Fig. 12 depicts the variations in local WSS along the curve length for various aneurysms at 0.3sec of the cardiac cycle. It can be seen that the WSS first decreases and then increases along the curve length. The minimum WSS has been noticed to occur at the centre of the affected region. However, in comparison with atherosclerosis, the WSS is significantly lower in aneurysms.

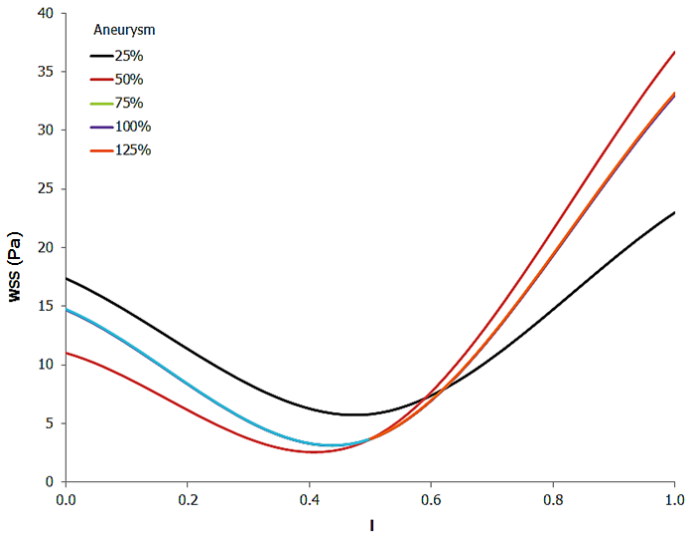

(a)

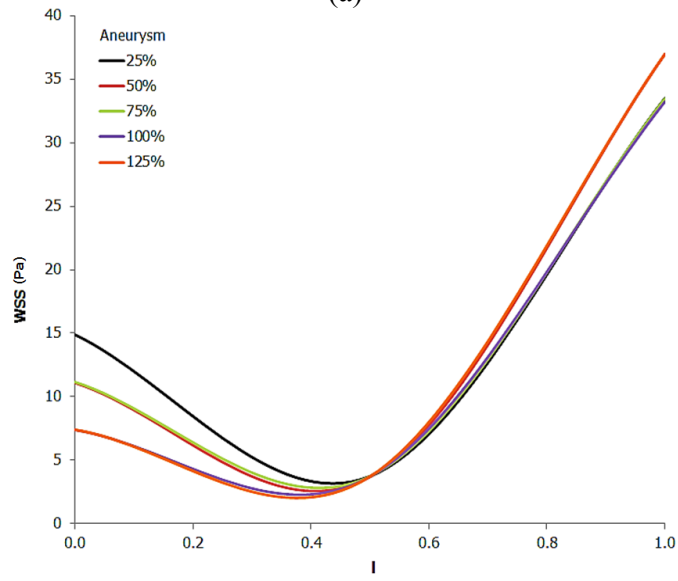

(b)

Figure 12. Variations in WSS for different Aneurysms at 0.3sec (a) 4mm (b) 8mm

Figure 13 depicts the variations in normalised WSS during one complete cardiac cycle, for various aneurysms considered in the present study. It can be seen that as the severity of the aneurysm increases, normalised peak WSS also increases.

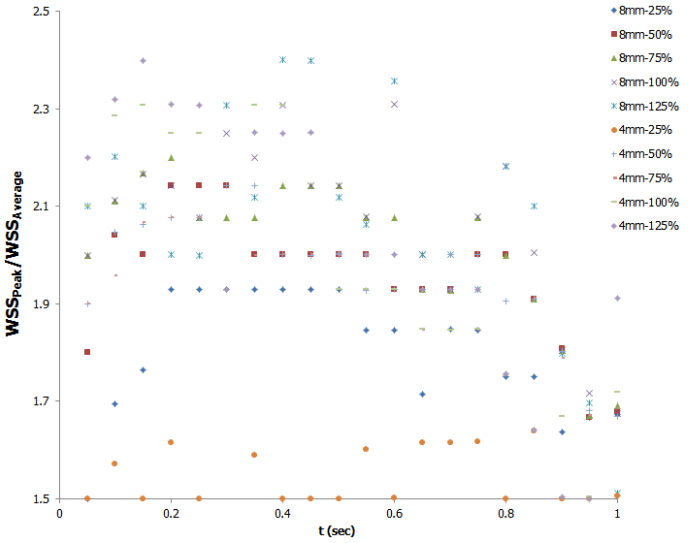

Figure 13. Variations in normalised peak WSS during a cardiac cycle for various aneurysms

The results presented in Fig. 13 have been used to develop a novel expression for the prediction of normalised peak WSS acting on the region affected by aneurysm by including geometric and flow parameters.

$$\frac{WSS_{Peak}}{WSS_{Aveage}} = 1 + \left(\frac{0.26 \left(\frac{L}{d}\right)^{0.188} AN^{0.258}}{\left(\frac{t}{t_{avg}}\right)^{0.1}} \right) \quad (4)$$

Where L is the length of region affected by aneurysm, d corresponds to the diameter of the carotid bifurcation and AN corresponds to severity of aneurysm (in %). It can be seen that, for the prediction of normalised peak WSS, severity of aneurysm is 37%and 158% more significant than L/d ratio and time respectively. Figure 14 presents the validity of Eq. (4). It can be seen that more than 85% of the data obtained from CFD, lies within ±10% error band of Eq. (4). Hence, Eq. (4) predicts the normalised peak WSS in the region affected by aneurysm, at a given time during a cardiac cycle, with reasonable accuracy.

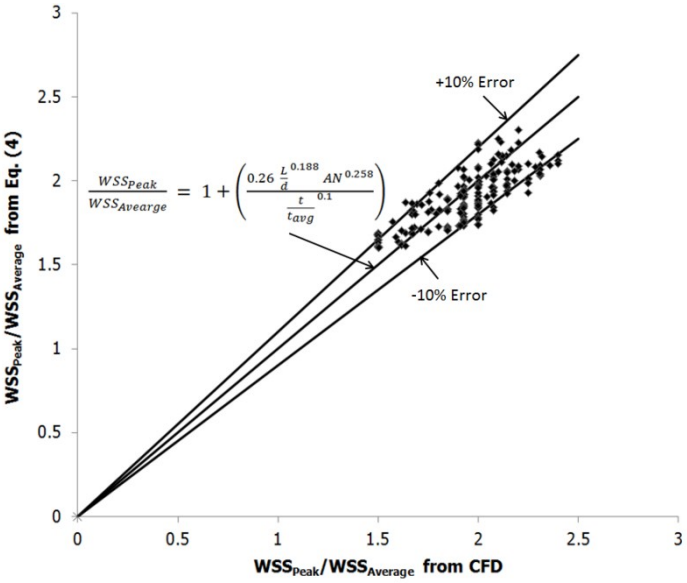

Figure 14. Validation of Eq. (4)

4. CONCLUSION

A numerical study of atherosclerosis and aneurysms using CFD has been presented. Realistic models of human carotid bifurcations have been developed with various severities of stenosis and aneurysm. It has been shown that local WSS is a better representation of the flow field nearby the walls of the affected region, as compared to time or area averaged average WSS. In case of atherosclerosis, maximum WSS occurs at the entrance of the throat. It has been concluded that as the severity of the stenosed region increases, the WSS increases up to a certain limit of stenosis, after which flow readjusts within the bifurcations. Furthermore, it has been shown that in case of aneurysms, the local WSS first decreases and

then increases in the affected region. WSS in aneurysms is considerably lower than observed for various atherosclerotic conditions. Novel expressions have been developed for both atherosclerosis and aneurysms that predicts the normalised peak WSS acting on the walls of the affected region.

REFERENCES

[1] Jiang, Y., Kohara, K., Hiwada, K.., 2000.Association between risk factors for atherosclerosis and mechanical forces in carotid artery, Stroke; a Journal of Cerebral Circulation31 2319 – 2324.

[2] Steinman, D. A., Thomas, J. B., Ladak, H. M., Milner, J. S., Rutt, B. K., Spence, J. D., 2002. Reconstruction of Carotid Bifurcation Hemodynamics and Wall Thickness Using Computational Fluid Dynamics and MRI, Magnetic Resonance in Medicine 47 149 – 159.

[3] Dong, J., Wong, K. K. L.,Tu, J., 2013.Hemodynamics analysis of patient-specific carotid bifurcation: A CFD model of downstream peripheral vascular impedence, International Journal for Numerical Methods in Biomedical Engineering, 29476 – 491.

[4] Marshall, I., Zhao, S., Papathanasopoulou, P., Hoskins, P., Xu, X. Y., 2004. MRI and CFD studies of pulsatile flow in healthy and stenosed carotid bifurcation models, Journal of Biomechanics 37 679 – 687.

[5] Martin, D., Zaman, A., Hacker, J., Mendelow, D., Birchall, D., 2009. Analysis of hemodynamic factor involved in carotid atherosclerosis using computational fluid dynamics, The British Journal of Radiology 82 33 – 38.

[6] Milos, R., M., Dejan, P., Nenad, F., 2011.Mining Data from CFD Simulation for Aneurysm and Carotid Bifurcation Models, In: 33rd Annual International Conference of the IEEE EMBS, Boston, Massachusetts, U.S.A.